Scientia Iranica F (2016) 23(6), 3163–3174

SCIENTIA IRANICA

Sharif University of Technology
Scientia Iranica
Transactions F: Nanotechnology
www.scientiairanica.com

Research Note

Facile templateless fabrication of ZnO nanostructures: A consideration of several parameters

S. Ghasaban[a], M. Atai[a,*], M. Imani[b] and A. Tarlani[c]

a. *Department of Polymer Science, Iran Polymer and Petrochemical Institute, Pajoohesh Blvd, Karaj Hwy, Tehran, P.O. Box 14965-115, Iran.*
b. *Department of Novel Drog Delivery Systems, Iran Polymer and Petrochemical Institute, Pajoohesh Blvd, Karaj Hwy, Tehran, P.O. Box 14965-115, Iran.*
c. *Inorganic Nanostructures and Catalysts Research Laboratory, Chemistry and Chemical Engineering Research Center of Iran, Pajoohesh Blvd, Karaj Hwy, Tehran, P.O. Box 14968-13151, Iran.*

Received 9 February 2016; received in revised form 12 June 2016; accepted 29 August 2016

KEYWORDS
Hydrothermal reaction;
Zinc oxide;
Nanostructures;
Morphology.

Abstract. ZnO nanostructures were formed via a hydrothermal reaction mechanism between simple anionic (ammonia or sodium hydroxide) and cationic (zinc acetate dehydrate) precursors without using any organic templates. Effects of the reaction conditions, including the initial solution pH, type and concentration of the anionic and cationic precursors, and the reaction time and temperature, on the nanostructure particle size and morphology were investigated. The nanostructures formed were analyzed by powder X-ray diffraction, energy dispersive X-ray analysis, and scanning electron microscopy. According to the results, the morphology of the nanostructures is highly pH-dependent. Needle-like nanostructures were formed using ammonia at initial solution pH value around 9, but plate-like nanostructures were formed using NaOH at pH value around 13, regardless of the reaction time or temperature. The precursors concentration could not be considered as an independent parameter per se as it consequently changes the reaction medium pH, which affects the morphology in turn. In general, increasing the reaction time and temperature increased the mean particle size of the nanostructures with no significant change in their morphology. It was found that the nanostructure morphology changes from nanoneedle to star-like at higher addition rates of ammonia.

© 2016 Sharif University of Technology. All rights reserved.

1. Introduction

In the recent years, nanostructures have attracted significant attention from both academic and industrial communities due to their enhanced characteristics in comparison to their counterpart micro-sized particles. Among these, zinc oxide (ZnO) nanostructures are the subject of intense interest due to their specific properties and widespread applications [1,2]. ZnO is a polar crystal, which possesses *n*-type semiconductor property with a wide band gap (3.3 eV) and large exciton binding energy (60 meV) [2]. It is also an environment-friendly material with piezoelectric capability and significant antibacterial and antifungal characteristics [3-6]. These characteristics make it an attractive choice for a wide range of high-tech applications such as gas sensors, varistors, transducers, solar cells, optical coatings, photocatalysis, and healthcare products such as lotions, ointments, creams, textiles, and antibacterial coatings for surfaces and biomedical devices [7,8].

*. *Corresponding author. Tel.: +98 21 48662446;*
E-mail addresses: S.Ghasaban@ippi.ac.ir (S. Ghasaban); M.Atai@ippi.ac.ir, (M. Atai); M.Imani@ippi.ac.ir (M. Imani); tarlani@ccerci.ac.ir (A. Tarlani)

The properties of ZnO are strongly dependent on its crystallinity, shape, and size [9]. These properties are determined by the synthesis conditions, e.g. the reaction temperature, concentration of reactants, and the type of capping agents used [2]. Several methods have been employed for synthesis of ZnO particles with different characteristics. The methods can be broadly classified into two main categories of vapor phase (physical vapor deposition, chemical vapor deposition, thermal oxidation of pure Zn, etc.) and solution phase (sol-gel route, spray pyrolysis for growth of thin film, electrophoresis, chemical precipitation, etc.) methods [1].

Hydrothermal reaction is one of the most commonly used methods for synthesis of nanoparticles, which can be performed in a closed system at a high autogenously formed pressure. Such harsh conditions enhance the reactivity of reactant species and result in a greatly reduced temperature required for preparing ceramic powders. In addition, the evaporation of volatile species can be suppressed, and stoichiometry of the reactions can be maintained during the reaction course. This method has also several other advantages such as providing a one-step synthetic route, simplicity, lower degree of particle aggregation, high purity of the products, being non-polluting, availability of low-cost precursors, relatively low temperatures needed, and narrow particle size distribution of the resulting particles. Furthermore, the method allows controlling the morphology and size of the resulting nanoparticles by changing the reaction conditions. Moreover, the hydrothermal method is consistent with green chemistry requirements due to the lower temperatures used during the reaction in water under a sealed environment [1,10-13].

Many reports are in hand for the synthesis of zinc oxide in the presence of organic assembling and structure-directing agents such as cetyltrimethylammonium bromide (CTAB), sodium sulfate, Sodium Dodecyl Sulfate (SDS), sodium bis (2-ethylhexyl) sulfosuccinate, polyethylene glycol, polyethylene imine, and ethanol amine [14-22]. The organics, however, should be removed later on from the sample to obtain a pure product. These materials also raise the cost of the production of zinc oxide. Therefore, usage of sodium hydroxide and ammonia as simple precipitating agents has been widely considered. However, tuning the morphology and the phase structure strongly depends on the ratio of reactants, temperature, time, etc. [2]. Usually, preparing zinc oxides in the presence of sodium hydroxide and ammonia suffers from obtaining variform and uniform structures.

In this study, a facile route is adopted for the controllable synthesis of different zinc oxide architectures in hydrothermal conditions without using any organic template moieties. From the various conditions such as time, temperature, pH, type and concentration of precursors, and the addition rate of anion precursor, only two or three factors have been considered in previous reports, which have led to one or two different structures [11,12,23,24]. In this study, all factors were applied and different morphologies were obtained.

2. Experimental method

2.1. Synthesis

All chemicals were of analytical grade and were used without further purification. To obtain the ZnO nanostructures, 0.25-0.5 g of zinc acetate dihydrate ($Zn(CH_3COO)_2.2H_2O$, Sigma Aldrich) was dissolved into 25 mL of deionized (DI) water as zinc cation source (solution (I)). In some batches, ammonia (NH_3, 25 wt.%, Merck, Germany) was dissolved into 5 mL of DI water as hydroxide anion precursors (solution (II)). In the others, 1 g of sodium hydroxide (NaOH) pellets (Merck, Germany) was dissolved into 15 mL of DI water as hydroxide anion precursors (solution (II)). Solution (II) was added into solution (I) while solution (I) was stirring. Then, DI water was added to extend the whole DI water to 50 mL. The pH of the resulting mixture was measured after 5 min of stirring. The final suspension was transferred to a 100-mL Teflon-lined stainless steel autoclave and held in an oven for fixed temperature in the range of 120-160°C and the reaction was allowed to proceed for different durations of time between 2-24 h. Finally, the autoclave was cooled down to ambient temperature. ZnO nanocrystals were synthesized at a pH value of 9-13. Table 1 shows the different synthesis conditions and run numbers.

2.2. Characterization

The samples were characterized thoroughly using different techniques. XRD was performed on an X'Pert MPD X-ray diffractometer (Philips, Netherlands) with monochromatized CuKα (λ = 1.54056 Å) incident radiation. XRD patterns were recorded from 20 to 90° (2θ) with a scanning step of 0.02°. The size distribution, morphology, and the composition of the samples were analyzed by SEM (SEM, Vega\\, TESCAN, Czech Republic) and EDXA (EDXA, INCA, Oxford Instruments Co., UK). All particle sizes were determined by image analysis using ImageJ 1.44p software (National Institute of Health, USA).

3. Results and discussion

Figures 1 and 2 show the XRD pattern and EDXA of ZnO nanostructures obtained from run 15. In fact, this sample was selected as a model from different runs. The results show the presence of crystalline material and all the XRD peaks can be indexed by hexagonal wurtzite phase of ZnO (JCPDS card no.

Table 1. Different synthesis conditions and sample codes.

Run	Zinc acetate (g)	Anion precursor	Temperature (°C)	Time (h)	pH
1	0.5	NH_3 (0.7 mL)	120	2	8.82
2	0.5	NH_3 (0.7 mL)	120	13	8.95
3	0.5	NH_3 (0.7 mL)	120	24	8.94
4	0.5	NH_3 (0.7 mL)	120	24	8.95
5	0.5	NH_3 (0.7 mL)	160	13	8.96
6	0.25	NH_3 (0.7 mL)	120	13	9.38
7	0.25	NH_3 (0.7 mL)	120	24	9.45
8	0. 5	NH_3 (0.7 mL)	120	6	9.01
9	0. 5	NH_3 (1.4 mL)	120	13	9.56
10	0.5	NH_3 (0.35 mL)	120	13	7.05
11	1.0	NH_3 (0.7 mL)	120	13	6.95
12	0.5	NaOH (1 g)	120	24	13.14
13	0.5	NaOH (1 g)	120	13	13.03
14	0.5	NaOH (< 1 g)	120	6	9.06
15	0.5	NaOH (1 g)	160	13	~ 13
16	0.5	NaOH (1 g)	160	24	13.05
17	0.5	NaOH (1 g)	120	2	13.08
18	0.5	NaOH (1 g)	120	6	13.11

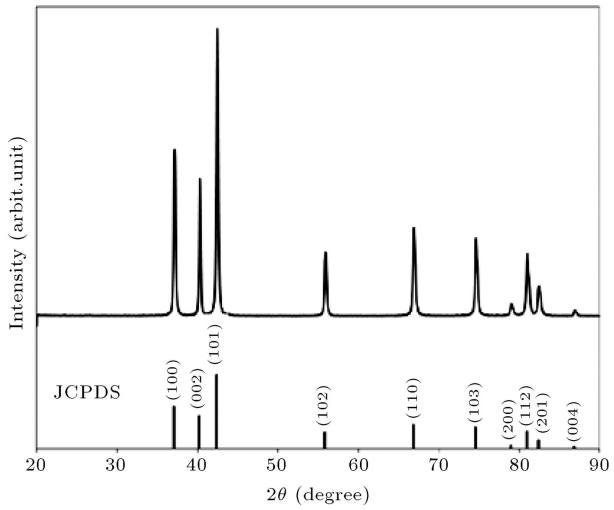

Figure 1. XRD results of ZnO nanostructures obtained from run 15 (see Table 1).

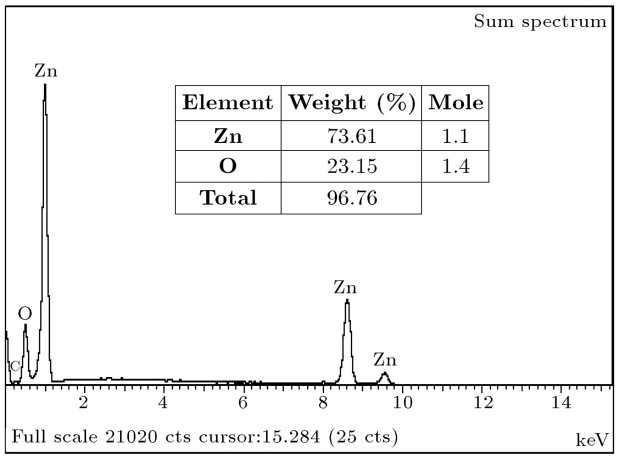

Figure 2. EDXA results of ZnO nanostructures obtained from run 15 (see Table 1).

36-1451, $a = 3.249$ Å, $c = 5.206$ Å). The peaks are sharp and strong, suggesting that the product is highly crystallized. The sharp peaks at diffraction angles of 37.12, 40.25, and 42.41 correspond to the (100), (002), and (101) diffraction planes, respectively. These nanostructures show their orientation of crystal growth along (101) plane. No other peak related to zinc and other impurities were detected in the pattern, which further confirms that the synthesized powders are pure ZnO.

The crystallite size (L) of the particles was determined from the measurement of the XRD line broadening using different methods. One of them is Scherrer equation, as follows [25]:

$$L = \frac{K\lambda}{\beta_S \cos\theta} \rightarrow \cos\theta = \left(\frac{K\lambda}{L}\right)\left(\frac{1}{\beta_S}\right), \quad (1)$$

where L is crystallite size in nm, λ is the radiation wavelength (1.54056 Å for CuKα) in nm, β_S is the Full Width at the Half Maximum (FWHM) in radian, θ is the diffraction angle (peak position), and K is the shape factor ($0.89 < K < 1$ here 0.94). To obtain real broadening of the sample, it is necessary to determine

the instrumental broadening and correct the measured β as follows [25]:

$$\beta_S^2 = \beta_{\text{measured}}^2 - \beta_{\text{instrumental}}^2. \quad (2)$$

According to Scherrer equation, by plotting $\cos\theta$ versus $(1/\beta_S)$, the crystallite size is extracted from the slope of fit line. Based on this method, the crystallite size of ZnO nanostructures is calculated 55.69 nm.

The other method is the Williamson-Hall (W-H) method. The W-H method does not follow $(1/\cos\theta)$ dependency unlike the Scherrer equation; instead, it varies with $\tan\theta$. By addition of size and strain broadening in the analysis, the fallowing equation is achieved [25]:

$$\beta = \beta_S + \beta_D, \quad (3)$$

$$\beta = \left(\frac{K\lambda}{L\cos\theta}\right) + 4\varepsilon\tan\theta \rightarrow \beta\cos\theta = \frac{K\lambda}{L} + 4\varepsilon\sin\theta. \quad (4)$$

Now, by plotting $\beta\cos\theta$ versus $4\sin\theta$, the crystallite size is determined from the intercept equal to 49.93 nm.

As it can be seen in EDXA analysis, the strong peaks attributed to Zn and O were found in the spectrum. Also, it was found that the Zn:O ratios in our nanostructures were close to the stoichiometric atomic ratio (Zn:O=1.1:1.4).

Figures 3 and 4 display SEM images of samples synthesized using two kinds of anionic precursors in different conditions listed in Table 1. Effects of different hydrothermal conditions such as time, temperature, pH, type and concentration of precursors, and the addition rate of anion precursor can be evaluated by analyzing SEM images as fallows. It is notable that due to absence of any surfactants, as templates, in the present work, the morphological evolution of ZnO products is obtained solely by hydrothermal reaction conditions and is dependent upon the concentration of the obtained $Zn(OH)_4^{2-}$. Although it was difficult to exactly find out the growth mechanism of ZnO based on the present experiments and the previous reports [11,23,24,26-28], we tried to explain how different morphologies with different sizes were formed.

3.1. Growth mechanism of ZnO nanostructures

To interpret the effect of hydrothermal conditions, especially pH and concentration of precursors, on size and morphology of the synthesized nanostructures, understanding the growth mechanism of ZnO is necessary. Several growth mechanisms are proposed to describe aqueous, chemical solution deposition reaction. The most important one for a single crystal is the so-called Ostwald ripening process [23]. Ostwald ripening is a physical phenomenon, which refers to the growth of larger crystals from those of smaller sizes which have a higher solubility than the larger ones [29]. This is a spontaneous process which happens because larger crystals are more energetically favored than smaller crystals. In this case, first, the nucleation of tiny crystallites, which are kinetically favored, is initiated in a supersaturated medium and, then, it is followed by the growth of larger particles, which are thermodynamically favored [23].

Layek et al. proposed a comprehensive mechanism describing nanoparticle formation in solution using a combination of experimental work and mathematical modeling. The mechanism includes the consecutive stages consisting of nucleation of ZnO nanocrystals and growth by molecular diffusion (I), interparticle coagulative-growth via oriented attachment (II), and interparticle growth by Ostwald ripening (III) [26].

Understanding the growth mechanism for varieties of ZnO morphologies still needs further improvement, but it can be explained in more details according to the findings of other researchers and our own results. The reaction starts from the making precursor solutions in pure water. The aqueous solutions of zinc acetate include the following chemical equilibria. It is notable that Zn^{2+} ions are the main zinc species in solution due to the weak hydrolyzing ability of CH_3COO^- ions [24].

$$Zn(CH_3COO)_{2(s)} + H_2O_{(l)} \leftrightarrow Zn^{2+}_{(aq)} + 2CH_3COO^-_{(aq)} + H_3O^+_{(aq)}. \quad (5)$$

Dissolving NaOH or ammonia in pure water separately results in OH^- ions. According to Xu et al., after adding the anion precursor (sodium hydroxide or ammonia) solution to cation precursor (zinc acetate) solution, the fallowing chemical equilibrium is reached at room temperature [24]:

$$Zn^{2+}_{(aq)} + 2OH^-_{(aq)} \leftrightarrow Zn(OH)_2 \downarrow. \quad (6)$$

By further increase in the anion precursor concentration, the intermediate product $Zn(OH)_2$ dissolves in the alkali solution and forms complexes of $Zn(OH)_4^{2-}$ in the solution. When the concentration of anion precursor solution increases more, the $Zn(OH)_4^{2-}$complexes are surrounded by a large amount of OH^- ions [24]:

$$Zn(OH)_2 + 2OH^-_{(aq)} \leftrightarrow Zn(OH)^{2-}_{4\ (aq)}. \quad (7)$$

Thus, $Zn(OH)_2$ is created from olation of Zn^{2+} in basic media. Subsequently, in hydrothermal process, oxolation of $Zn(OH)_2$ leads to ZnO production [30]:

$$Zn(OH)_2 \leftrightarrow ZnO + H_2O. \quad (8)$$

Wang et al. also proposed the following equation [11]:

$$Zn(OH)_4^{2-} \leftrightarrow ZnO + 2OH^- + H_2O. \quad (9)$$

To explain in detail, Xu et al. suggest that due to heat convection, diffusion of ions, and deregulation movement among molecules and ions in the solution, the clusters of $Zn_xO_y(OH)_z^{(z+2y-2x)-}$ are formed by dehydration reaction of $Zn(OH)_4^{2-}$. When the particle size of these clusters reaches a certain value (supersaturation state), the ZnO nucleus is formed and then ZnO is precipitated [24].

Aneesh et al. state that the $Zn(OH)_2$ precipitates strongly tend to be transformed into ZnO crystals during the hydrothermal process due to the lower solubility of ZnO than $Zn(OH)_2$ under the hydrothermal conditions. They believe that at the initial stage of the process, Zn^{2+} and OH^- concentrations are relatively higher so that the crystal growth in different directions is probable. When Zn^{2+} and OH^- concentrations reach the super saturation degree of ZnO, ZnO begins to be nucleated and the crystal growth is initiated [31].

In addition, Nicholas et al. prove that the hydrothermal growth of ZnO occurs via the initial precipitation of ε-$Zn(OH)_2$, which is subsequently dehydrated and forms Wurtzite ZnO [27].

Furthermore, Sun et al. and Mohajerani et al. declare that when zinc ions and hydroxyl ion concentrations increase in alkali solutions, $Zn(OH)_2$ is the prominent composition formed *in situ via* the reaction between Zn^{2+} and OH^-. Subsequently, in the hydrothermal condition, $Zn(OH)_2$ can be dehydrated to produce ZnO [14,28]. Similar to Xu et al., Mohajerani et al. assert that during the subsequent hydrothermal process, $Zn(OH)_2$ colloids dissolve into Zn^{2+} and OH^- and culminate in the formation of $Zn(OH)_4^{2-}$ growth units by reaching the supersaturation of ZnO [28].

According to the above mechanism, all the growth, dissolution, and Ostwald ripening processes impress particle size. It can be concluded that in hydrothermal reaction conditions, if the growth reaction is dominant, the particle size will increase and if the dissolution is overbearing, i.e. when the pH is high, the particle size will decrease (according to Eq. (9)). Also, it is deduced that the initial zinc species, their environment in the reaction medium, and growth unit concentration affect the nucleation and growth of ZnO crystal and, thus, the morphology of as-formed ZnO powder. Therefore, controlling the concentration of precursors and pH of the initial solution before hydrothermal process is essential for controlling the final particle size and morphology.

3.2. Effect of hydrothermal reaction time and temperature

From SEM micrographs shown in Figure 3, it is evident that all of the samples that are prepared by using ammonia as an anionic precursor mainly consist of ZnO needle-like morphologies and the particles are almost uniform. The obtained morphology by using sodium hydroxide, as anionic precursor, however, is uniform plate-like as it can be observed in Figure 4.

In addition to the reaction medium properties, based on our results, reaction time and temperature play important roles in determining ZnO nanoparticle size. Figure 5 demonstrates the effect of hydrothermal reaction time and temperature on the particle size of nanostructures according to particle size measurements by image analysis for 100 particles selected randomly in SEM micrographs.

As can be seen in Figure 5, samples obtained from 1, 8, 2, and 3 test runs were grown using NH_3 and 0.5 g $Zn(CH_3COO)_2.2H_2O$ at constant temperature of 120°C for 2, 6, 13, and 24 h, respectively. As shown in the same figure, there is a slight increase in particle size in the range of 210-260 nm by increasing the hydrothermal time from 2 to 6 h. However, the particle size decreases to 125 nm by increasing reaction time to 13 h. By further increase in the reaction time to 24 h, the particle size increases to *ca.* 295 nm.

Samples 6 and 7 were grown using NH_3 for 13 and 24 h, respectively, at a constant temperature of 120°C and using 0.25 g $Zn(CH_3COO)_2.2H_2O$. Similar to samples 2 and 3, the particle size increases from 255 nm to 700 nm by increasing hydrothermal time from 13 to 24 h (see Figure 5).

Samples 17, 18, 13, and 12 were raised for 2, 6, 13, and 24 h, respectively, at constant temperature of 120°C, and samples 15 and 16 were synthesized for 13 and 24 h, respectively, at constant temperature of 160°C, using 1 g of NaOH and 0.5 g of $Zn(CH_3COO)_2.2H_2O$. It is observed that at 120°C, by increasing time, the particle size increases; but, at 160°C, the particle size does not change significantly (Figure 5). It seems that at higher temperature (160°C), the rates of dissolution and formation of the crystal equilibrates.

Thus, as a final conclusion, it can be inferred that at constant temperature of 120°C and using 0.25 or 0.5 g of $Zn(CH_3COO)_2.2H_2O$, irrespective of the type of anion precursor used, by increasing the hydrothermal reaction time from 2 to 6 h (samples obtained from 1 and 8 or 17 and 18 test runs), the particle size increases. However, the particle size decreases when the time increases from 6 to 13 h, as it is evident by comparing samples obtained from 8 and 2 or 18 and 13 test runs. It can be proposed that by increasing the reaction time from 2 to 6 h, crystal growth is the dominant reaction; but, when it reaches 13 h, ZnO dissolution in the media takes place, which results in reduction of particle size. By prolonging the reaction time to 24 h (see samples 2 and 3, 6 and 7, or 13 and 12 in Figure 5), the particle size increases again. It could be concluded that there are still enough nucleation units, even after 24 h of reaction time.

In other studies, different findings are also re-

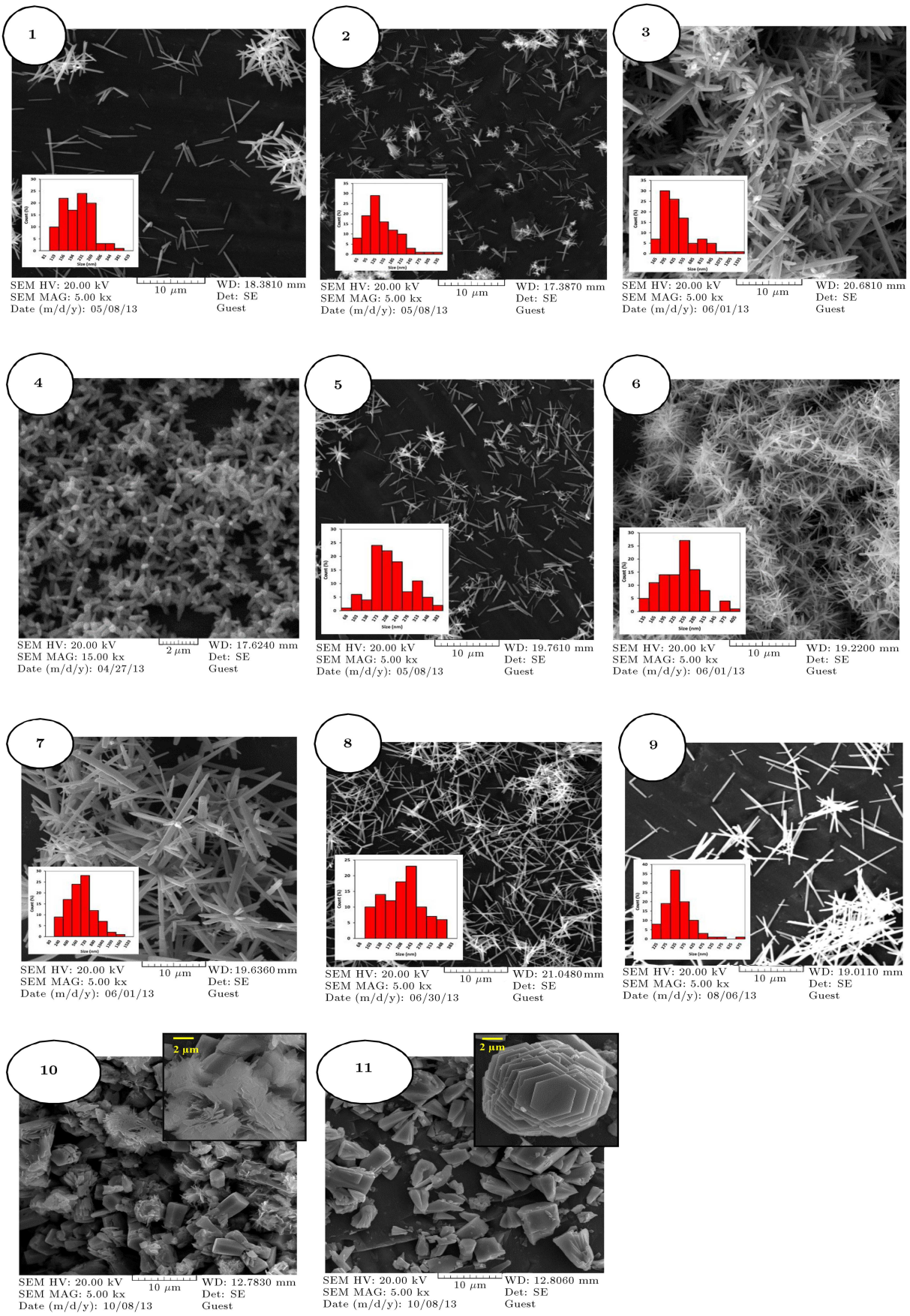

Figure 3. SEM micrographs of samples prepared using NH_3 as anionic precursor (runs 1 to 11).

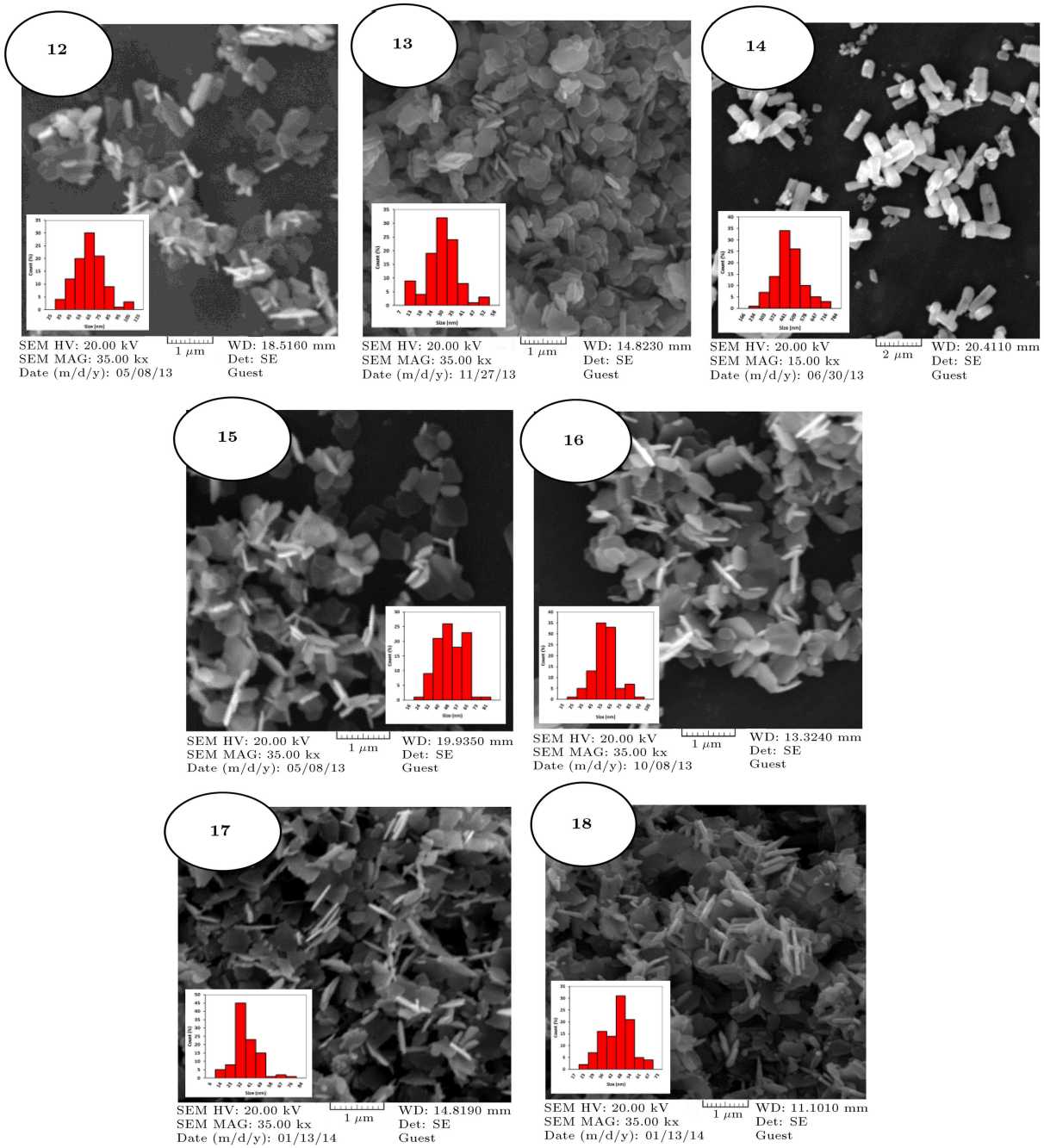

Figure 4. SEM micrographs of samples prepared using NaOH as anionic precursor (runs 12 to 18).

ported. For instance, Lu et al. reported that no difference in the morphology and the particle size (around 1.3 μm) of ZnO synthesis at 100°C was observed by increasing the hydrothermal reaction time from 0 to 2 h [12]. But, according to the evolution process of the surface morphology, Wang et al. indicated that the crystallinity and size of crystals increased when the reaction time increased from 4 to 8 and 16 h at constant temperature of 120°C. The morphology changed from pyramid-like tip rods to lath-like ZnO particles through the coalescence of two hexagonal rods, which were closely parallel to each other [11]. From XRD results of Aneesh et al., it can be concluded that the grain size increases from 7 to 17 nm as the growth time increases from 6 to 12 h at 200°C using 0.3 M NaOH [31]. Similar to our results, Polsongkram et al. noticed that the shapes of the ZnO nanorods were hexagonal and were independent of the deposition time, when changing from 15 to 30 min and then 60 min, using $ZnNO_3$-0.04 M: HMT-0.025M at 75°C. However, the nanorod size increased and the density decreased by increasing the deposition time due to the Ostwald ripening [23].

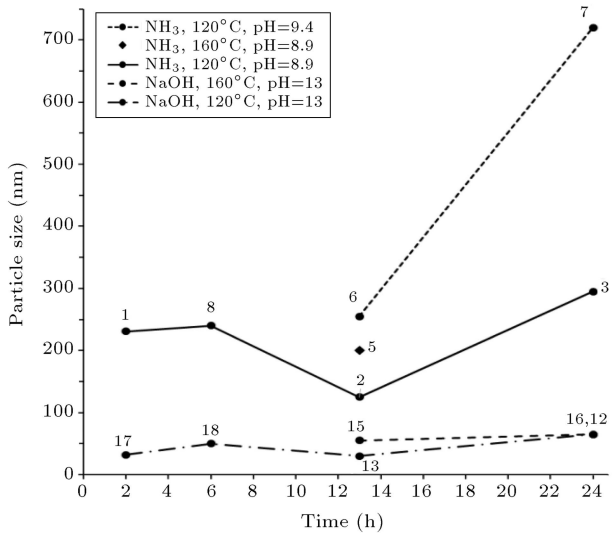

Figure 5. Particle size of ZnO nanoparticles *vs.* time (numbers next to each symbol show the runs).

By comparing samples 2 and 5, which are synthesized for 13 h at 120 and 160°C, respectively, by using ammonia as an anion precursor (Figure 5), it can be found that by increasing hydrothermal temperature, the particle size increases from 125 to *ca.* 200 nm; but the morphology is needle-like in both samples. Samples in runs 12, 16, 13, and 15 were synthesized using sodium hydroxide as an anion precursor. The first two ones were prepared at 120 and 160°C for 24 h, respectively, and the second two at 120 and 160°C for 13 h. All samples had the same plate-like morphology. Also, it can be found that at 24 h, by increasing temperature, particle size did not change significantly (*ca.* 65 nm); but, at 13 h, by increasing temperature, growth in the particle size was observed. In fact, when the time is prolonged to 24 h, the particles grow at the maximum rate based on the concentration of initial precursors and, in this condition, increasing temperature has no effect on the particle size.

Same as for hydrothermal reaction time, controversial results have been reported for the effect of temperature on particle size and morphology of ZnO by different authors. For example, Gavrilov et al. investigated hydrothermal synthesis of ZnO using a zinc metal substrate in the presence of organic reagents such as ethylene diamine (EDA) and formamide. They found out that decreasing the reaction temperature from 220 to 180 and then to 140°C leads to decrease in the mean rod size, i.e. the rod width changes from *ca.* 1.4 to 1.2 and 0.8 μm, respectively, which is very close to our findings [13]. Also, Aneesh et al., who calculated the average grain size by Scherrer equation using XRD patterns, observed an increase from 7 to 16 nm as the temperature increased from 100°C to 200°C at 0.3 M NaOH concentration for a growth time of 6 h [31]. Sun et al. utilized the reaction temperatures of 180, 140, and 28°C. In spite of the results reported by some other researchers, their findings indicated that ZnO nanoparticle morphology changed from flower-like to regularly nanorods with larger diameter and length by decreasing reaction temperature from 180 to 140°C. At room temperature, only a bulk of hexagonal ZnO materials with large diameters was obtained [16]. Lu et al. showed that raising the hydrothermal reaction temperature to more than 100°C slightly reduced the particle size of ZnO powder in accordance to Sun et al. data [12]. Same as the two groups of researchers above, Polsongkram et al. believed that ZnO nanorod morphology and surface-to-volume ratio were most sensitive to temperature. They showed that reducing temperature from 95 to 75 and then 60°C resulted in increasing ZnO rod diameter from 150 to 500 nm and larger thick branched rods [23]. Besides, Sondergaard et al. showed that no ZnO was observed at reactor temperatures below 75°C and only the precursor phase was recorded according to XRD patterns. Based on their results, the particle size and morphology are highly temperature-dependent. At a reactor temperature of 122°C, anisotropic particles with a maximum length of 1 μm were formed, whereas at temperatures above 200°C, isotropic particles of around 25 nm were produced. They found out a definite trend by Rietveld refinement of XRD data, which ascertained that low temperatures resulted in the particles with elongated diamond shape, while at higher temperatures, the particles appeared in a more isotropic crystallite domain shape. At around 210°C and up to 390°C, the morphology does not change significantly. The samples synthesized at 90°C deviate from this general trend, but refinement of these data is less reliable as the sample was not pure phase [32].

3.3. Effect of initial solution pH

Changing the type and amount of initial materials including NH_3, NaOH, or zinc salt can surely end to different pH values for the initial solution. Figure 6 indicates the effect of initial solution pH values on particle size of the ZnO nanostructures. As the nucleation and growth stages of ZnO formation depend on concentration of zinc hydroxide ions and supersaturation conditions during hydrothermal process, each factor changing the amount of Zn^{2+} or OH^- concentration will affect the growth mechanism and may change the size or morphology of ZnO nanoparticles.

All of the samples, which were prepared using NH_3 as anion precursor with the initial solution pH of about 9, ended in a needle-like morphology (see Figure 3). However, the nanostructures, which were performed via using NaOH as an anion precursor with the initial solution pH of *ca.* 13, resulted in a plate-like morphology (Figure 4). In all of these samples, different hydrothermal reaction conditions did not

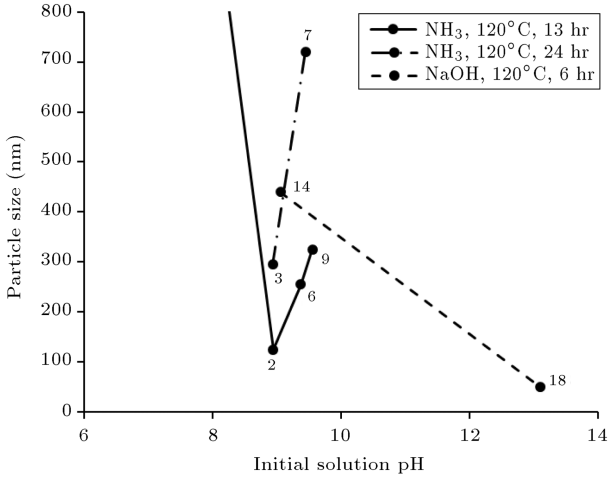

Figure 6. Particle size of ZnO powder *vs.* pH of the initial solution (numbers beside each dot show runs. Samples obtained in runs 10 and 11 have particle sizes more than 2000 nm).

affect morphology of ZnO nanoparticles significantly. Surface (001), which is often called the zinc-terminated face, is composed of zinc atoms and is one of the two polar faces normal to the *c*-axis [33]. It is the typical surface growth [23]. When ZnO nuclei are formed in the initial growth stage of crystals, ZnO crystals grow preferentially along the (001) direction to form rod-like or needle-like structures due to the higher growth rate along this direction [34]. Here, however, at the pH of *ca.* 13, the growth has proceeded along (101) nonpolar plane. It may be due to the covering of (001) plane by $[OH^-]$ functional groups, which are present at high concentration at this level of pH and prevent contact between the growth unit and the (001) crystal surface or the possibility of ZnO dissolution at higher pH according to Eq. (9).

Reducing the pH value to about 7 by using less NH_3 or more zinc salt in the same conditions like the cases of samples 10 and 11 drastically changed the morphology. The obtained products were much larger and had different morphologies such as rod-like, flower-like, and wedge-like (Figure 3). Samples 10 and 11 were synthesized at 120°C for 13 h. The former was performed using 0.5 g of $Zn(CH_3COO)_2.2H_2O$ and 0.35 mL of NH_3, and the latter was synthesized using 1 g of $Zn(CH_3COO)_2.2H_2O$ and 0.7 mL of NH_3. Decreasing the anion precursor or increasing zinc salt concentrations resulted in reduced initial solution pH to *ca.* 7 (Table 1). Thus, the initial solution was not alkali anymore. It is expected that decreasing pH value would result in more ZnO crystals according to Eq. (9) and their rapid growth would lead to the formation of irregular structures. Gavrilo et al. reported the same results for using non-ionic surfactants [13]. This may be also attributed to the diffusion of particles together during 13 h of hydrothermal reaction time as shown in inset images at higher magnification in SEM results of these samples (see Figure 3).

In addition, comparing sample 14, which is prepared using NaOH with initial solution pH of about 9, with other samples using NaOH as an anion precursor with initial solution pH of about 13 indicates that morphology of ZnO nanoparticles changes drastically from plate-like to larger rod-like particles by decreasing pH values regardless of hydrothermal reaction time and temperature. By reducing pH values and, in fact, decreasing $[OH^-]$ groups, the (001) plane covering effect of hydroxyl groups, as explained before, disappears, and ZnO crystals grow along the preferable (001) direction and form rod-like structures [34].

Samples 2, 6, 3, and 7 were synthesized at 120°C using ammonia as anion precursor. By comparing the first two ones (samples 2 and 6), which are prepared in 13 h using 0.5 and 0.25 g of $Zn(CH_3COO)_2.2H_2O$, respectively, it is evident that decreasing zinc salt concentration ($[Zn^{2+}]$) results in increasing pH from 8.95 to 9.38 and particle size from 125 to 255 nm (Figure 6). It is similar for the second two ones (samples 3 and 7), which are prepared in 24 h using 0.5 and 0.25 g of $Zn(CH_3COO)_2.2H_2O$, respectively. This change, i.e. decreasing cation precursor concentration, is associated with a corresponding change in pH values from 8.94 to 9.45. The results showed that ZnO nanoparticle size increased from *ca.* 300 to 600 nm. Sample 9, which is prepared in the same condition with samples 2 and 6 (120°C, 13 h reaction condition), has initial pH of 9.56, due to higher concentration of NH_3. As it can be observed in SEM images (see Figure 3), the morphology is needle-like with lager diameter than that of sample 2 (325 *vs.* 125 nm). Since pH is an effective parameter in nucleation and growth, changing particle size and morphology is so expectable. In fact, according to our results, addition of anion precursor or decreasing cation precursor, both of which result in higher $[OH^-]$ concentration and pH, leads to increase in nanoparticle size; but, due to low change in $[OH^-]$ concentration, the morphology remains the same.

3.4. Effect of type and addition rate of anion precursor base

Samples 8 and 14 are grown at 120°C for 6 h using NH_3 and NaOH as anion precursors at the same pH value of *ca.* 9, respectively. It is obvious that the morphology changes from needle- to rod-like ZnO particles. As it was mentioned before, (001) polar plane is the preferable ZnO growth direction, which leads to rod-like ZnO nanostructures; but, suppression of symmetric growth of six (101) surfaces results in needle-like nanostructures [34].

In all of the samples, anion precursor was added to zinc salt solution dropwise, except for sample 4, which was prepared by adding ammonia solution into

zinc salt solution rapidly. As shown in SEM images (Figure 3), by comparing samples 3 and 4, which are different only in the addition rate of ammonia, the morphology changes from needle- to star-like. In fact, rapid addition of ammonia into zinc salt solution provides hydroxide anions very quickly, which results in a large amount of growth units of $Zn(OH)_4^{2-}$ and $Zn(NH_3)_4^{2+}$. Thus, during hydrothermal process, more growth units around the ZnO nuclei may lead to a faster growth kinetics, which cause sheet defects of the ZnO crystals in the initial growth stage and it is possible that the initial ZnO crystal has many polar (001) surfaces. Therefore, due to the preferential growth along the (001) direction, as the reaction goes on, star-shaped ZnO can be obtained [34].

4. Conclusion

Needle-like, plate-like, rod-like, and star-like ZnO nanostructures were obtained via simple hydrothermal reaction without using any template, catalyst, or surfactant. The considered parameters were zinc salt concentration, anionic precursor type, concentration and its addition rate to the zinc salt solution, and hydrothermal time and temperature. In conclusion, the most important factor in determining the final morphology of nanostructures is the initial solution pH. Using ammonia as anionic precursor with initial solution pH value of *ca.* 9 resulted in needle-like morphology and if it was rapidly added to zinc salt solution, star-like particles were obtained. Using sodium hydroxide instead of ammonia with initial solution pH value of about 13 led to plate-like ZnO nanostructures and by decreasing pH to about 9, rod-like morphology was achieved. The key factor in controlling morphology of ZnO is controlling the crystal growth and dissolution rates in specific directions and the concentration of growth units. Besides, hydrothermal time and temperature did not affect the morphology, but changed the particle size significantly.

References

1. Cioffi, N. and Rai, M., *Nano-Antimicrobials: Progress and Prospects*, Berlin Heidelberg, Springer-Verlag (2012).
2. Sharma, D., Rajput, J., Kaith, B.S., et al. "Synthesis of ZnO nanoparticles and study of their antibacterial and antifungal properties", *Thin Solid Films*, **519**(3), pp. 1224-1229 (2010).
3. Ann, L.C., Mahmud, S., Barkhori, S.K.M, et al. "Characterization of ZnO nanopowder and antibacterial response against Staphylococcus aureus under UVA illumination", *Advanced Materials Research*, **795**, pp. 148-152 (2013).
4. Xu, X., Chen, D., Yi. Z., et al. "Antimicrobial mechanism based on H_2O_2 generation at oxygen vacancies in ZnO crystals", *Langmuir*, **29**(18), pp. 5573-5580 (2013).
5. Kumar, R., Anandan, S., Hembram, K. and Narasinga Rao, T. "Efficient ZnO-based visible-light-driven photocatalyst for antibacterial applications", *ACS Applied Materials & Interfaces*, **6**(15), pp. 13148-13138 (2014).
6. Diez-Pascual, A.M. and Diez-Vicente, A.L. "ZnO-reinforced poly (3-hydroxybutyrate-co-3-hydroxy- valerate) bionanocomposites with antimicrobial function for food packaging", *ACS Applied Materials & Interfaces*, **6**, pp. 9822-9834 (2013).
7. Nair, M.G., Nirmala, M., Rekha, K. and Anukaliani, A. "Structural, optical, photo catalytic and antibacterial activity of ZnO and Co doped ZnO nanoparticles", *Materials Letters*, **65**(12), pp. 1797-1800 (2011).
8. Baruah, S. and Dutta, J. "Hydrothermal growth of ZnO nanostructures", *Science and Technology of Advanced Materials*, **10**(1), p. 013001 (2009).
9. Tarlani, A., Fallah, M., lotfi, B., et al. "New ZnO nanostructures as non-enzymatic glucose biosensors", *Biosensors and Bioelectronics*, **67**, pp. 601-607 (2014).
10. Ramimoghadam, D., Hussein, M.Z.B. and Taufiq-Yap, Y.H. "The effect of sodium dodecyl sulfate (SDS) and cetyltrimethylammonium bromide (CTAB) on the properties of ZnO synthesized by hydrothermal method", *International Journal of Molecular Sciences*, **13**(10), pp. 13275-13293 (2012).
11. Wang, H., Xie, J., Yan, K. and Duan, M. "Growth mechanism of different morphologies of ZnO crystals prepared by hydrothermal method", *Journal of Materials Science & Technology*, **27**(2), pp. 153-158 (2011).
12. Lu, C.-H. and Yeh, C.-H. "Influence of hydrothermal conditions on the morphology and particle size of zinc oxide powder", *Ceramics International*, **26**(4), pp. 351-357 (2000).
13. Gavrilov, A.I., Baranov, A.N., Churagulov, B.R. and Tretyakov "Zinc oxide nanorod arrays synthesized on zinc foil by hydrothermal route", *Doklady Chemistry*, **432**, pp. 155-158 (2010).
14. Sun, X.M., Chen, X., Deng, Z.X. and Li, Y.D. "A CTAB-assisted hydrothermal orientation growth of ZnO nanorods", *Materials Chemistry and Physics*, **78**(1), pp. 99-104 (2003).
15. Oliveira, A.P.A., Hochepied, J-F., Grillon, F. and Berger, M-H."Controlled precipitation of zinc oxide particles at room temperature", *Chemistry of Materials*, **15**(16), pp. 3202-3207 (2003).
16. Sun, G., Gao, M., Wang. Y., et al. "Anionic surfactant-assisted hydrothermal synthesis of high-aspect-ratio ZnO nanowires and their photoluminescence property", *Materials Letters*, **60**(21), pp. 2777-2782 (2006).
17. Gao, P., Ying, C., Wang, S., et al. "Low temperature hydrothermal synthesis of ZnO nanodiskarrays utilizing self-assembly of surfactant molecules at solid-liquid interfaces", *Journal of Nanoparticle Research*, **8**(1), pp. 131-136 (2006).

18. Duan, J., Huang, X. and Wang, E. "PEG-assisted synthesis of ZnO nanotubes", *Materials Letters*, **60**(15), pp. 1918-1921 (2006).

19. Tam, K.H., Cheung, C.K., Leung, Y.H., et al. "Defects in ZnO nanorods prepared by a hydrothermal method", *The Journal of Physical Chemistry B*, **110**(42), pp. 20865-20871 (2006).

20. Wang, X., Zhang, Q., Wan, Q., et al. "Controllable ZnO architectures by ethanolamine-assisted hydrothermal reaction for enhanced photocatalytic activity", *The Journal of Physical Chemistry C*, **115**(6), pp. 2769-2775 (2011).

21. Xu, C. and Gao, D. "Two-stage hydrothermal growth of long ZnO nanowires for efficient TiO_2 nanotube-based dye-sensitized solar cells", *The Journal of Physical Chemistry C*, **116**(12), pp. 7236-7241 (2012).

22. Zhu, S., Chen, X., Zuo, F., et al. "Controllable synthesis of ZnO nanograss with different morphologies and enhanced performance in dye-sensitized solar cells", *Journal of Solid State Chemistry*, **197**, pp. 69-74 (2013).

23. Polsongkram, D., Chamninok, P., Pukird, S., et al. "Effect of synthesis conditions on the growth of ZnO nanorods via hydrothermal method", *Physica B: Condensed Matter*, **403**(19), pp. 3713-3717 (2008).

24. Xu, H., Wang, H., Zhang, Y., et al. "Hydrothermal synthesis of zinc oxide powders with controllable morphology", *Ceramics International*, **30**(1), pp. 93-97 (2004).

25. Khorsand Zak, A., Abd Majid, W.H., Abrishami, M.E. and Yousefi, R. "X-ray analysis of ZnO nanoparticles by Williamsone Hall and size strain plot methods", *Solid State Sciences*, **13**(1), pp. 251-256 (2011).

26. Layek, A., Mishra, G., Sharma, A., et al. "A generalized three-stage mechanism of ZnO nanoparticle formation in homogeneous liquid medium", *The Journal of Physical Chemistry C*, **116**(46), pp. 24757-24769 (2012).

27. Nicholas, N.J., Franks, G.V. and Ducker, W.A. "The mechanism for hydrothermal growth of zincoxide", *Cryst. Eng. Comm.*, **14**(4), pp. 1232-1240 (2012).

28. Mohajerani, M.S., Lak, A. and Simchi, A. "Effect of morphology on the solar photocatalytic behavior of ZnO nanostructures", *Journal of Alloys and Compounds*, **485**(1), pp. 616-620 (2009).

29. Chun Zeng, H. "Ostwald ripening: a synthetic approach for hollow nanomaterials", *Current Nanoscience*, **3**(2), pp. 177-181 (2007).

30. Jolivet, J.-P., Henry, M. and Livage, J., *Metal Oxide Chemistry and Synthesis: From Solution to Solid State*, Wiley-Blackwell (2000).

31. Aneesh, P.M., Vanaja, K.A. and Jayaraj, M.K. "Synthesis of ZnO nanoparticles by hydrothermal method", in *NanoScience+ Engineering, International Society for Optics and Photonics* (2007).

32. Sondergaard, M., Bojesen, E.D., Christensen, M. and Iveresen, B.B. "Size and morphology dependence of ZnO nanoparticles synthesized by a fast continuous flow hydrothermal method", *Crystal Growth & Design*, **11**(9), pp. 4027-4033 (2011).

33. Golovko, D.S., Munoz-Espi, R. and Wegner, G. "Interaction between poly (styrene-acrylic acid) latex nanoparticles and zinc oxide surfaces", *Langmuir*, **23**(7), pp. 3566-3569 (2007).

34. Cho, S., Jung, S.-H. and Lee, K.-H. "Morphology-controlled growth of ZnO nanostructures using microwave irradiation: from basic to complex structures", *The Journal of Physical Chemistry C*, **112**(33) pp. 12769-12776 (2008).

Biographies

Samaneh Ghasaban was born in 1985 and is currently a PhD student of Polymer Engineering at Iran Polymer and Petrochemical Institute (IPPI). She received her BSc in Chemical Engineering with emphasis on Polymer Industry from Isfahan University of Technology (IUT) in 2007. Also, she graduated from IPPI with MSc degree in Engineering of Polymer Science and Technology, in 2009. For her PhD thesis, she is working on an antibacterial pressure-sensitive adhesive for skin-contact applications. Her research interest is polymer (nano)composites and adhesives for medical applications.

Mohammad Atai was born in 1967 and is a Professor of Polymer Engineering at Iran Polymer and Petrochemical Institute (IPPI). He graduated from Amirkabir University of Technology with an MSc degree in Polymer Engineering in 1994. Also, he received his PhD degree in Polymer Engineering in 2004 from IPPI. His research areas of interest include synthesis of polymers and (nano)composites, focusing on dental polymeric materials.

Mohammad Imani is an Associate Professor of Pharmaceutics at Novel Drug Delivery Systems (NDDS) Department of Iran Polymer and Petrochemical Institute (IPPI). He graduated in Pharmacy in 1996; then, he received a PhD degree in Pharmaceutics in 2002, prior to joining IPPI. His research interests include polymer synthesis and development, including new unsaturated aliphatic polyesters, furan resins, etc.; application of polymeric materials to develop controlled-release drug delivery devices; and tissue engineering.

Dr. Imani has engaged in some international research, focusing on development of novel drug-eluting

cochlear implant devices, and is an advisor to some companies of drug-eluting biomedical devices. His research has been funded by government agencies and corporations. He is a co-inventor of three US patent applications.

Aliakbar Tarlani was born in Tehran in 1976. He graduated with a BS in Applied Chemistry in 1999 at Tehran University and then received his MSc and PhD degrees in Inorganic Chemistry Field for his work on nano-metal and non-metal oxide chemistry and catalytic application of heteropoly acids with M. Abedini and M.M. Amini in 2007. In 2006, he spent a sabbatical period with J. Muzart at Université de Reims, working on development of some catalytic reactions. Now, he is Assistant Professor of Inorganic Chemistry in the Faculty of Chemical Processes Development, Chemistry & Chemical Engineering Research Center of Iran (CCERCI), working on new synthetic routes for the fabrication of inorganic nano materials with particular emphasis on their catalytic, sensor, drug-delivery, and green-chemistry applications.